EVALUATING THE EFFECT OF SHRINKAGE ON THE EFFECTIVE THERMAL CONDUCTIVITY OF A GLASS-REINFORCED PLASTIC

E. A. Artyukhin, V. A. Mamolov, and
A. V. Nenarokomov

UDC 536.24

Results are presented from experimental-theoretical determination of the temperature dependence of the effective thermal conductivity of a glass-reinforced plastic on the basis of solution of the inverse problem.

Reinforced plastics are in wide use in different thermally loaded structures. The intensive heating of such materials is accompanied by the occurrence of complex multistage processes resulting from thermal degradation of the binder. These processes in turn lead to changes in the structure, chemical composition, and physical properties of the composite and its shrinkage. The interrelatedness of the factors just mentioned makes it important to study the thermophysical properties of glass-reinforced plastics under nonsteady conditions approximating actual service [1].

One of the most effective approaches to solving this problem is to conduct experimental–theoretical studies based on analysis of empirical data by inverse-problem methods [2].

A boundary-value problem for a homogeneous heat conduction equation is usually used as a simple mathematical model which describes the heating of materials of complex composition. In such a model, thermal degradation of the material is usually considered by introducing effective thermophysical characteristics.

Inverse-problem methods have been used in [3-5], for example, to establish the effective thermophysical properties of materials of complex composition. Here, the effect of phenomena connected with shrinkage of the materials on the final results is usually ignored. The goal of the studies described in the present article was to evaluate the possible effect of shrinkage phenomena on the effective thermal conductivity determined from the solution of the inverse problem as a function of temperature.

In the solution of inverse problems, the initial data are the coordinates of the heat sensors in the test specimen and the results of nonsteady measurement of temperatures at these points. Temperatures inside the specimen are usually measured with thermocouples, and the coordinates of the latter are usually determined before the test by means of x-ray diffraction analysis.

To evaluate the possible effect of shrinkage of the test material on the results of a thermophysical experiment conducted under transient conditions, it is necessary to determine the thermophysical characteristics with and without allowance for the sensor displacements measured during the test and caused by shrinkage of the material. The effects of shrinkage are determined by comparing the results of analyses of data from the same given test by both of the methods just mentioned.

We will assume that heat sensors are installed at a certain number N + 2 of specimen points. During the test, in a certain coordinate system we record the change in the position of the sensors over time $Y_i(\tau)$, $i = \overline{1, N+2}$ and we measure the temperature

$$T_{\text{expt}}(Y_i(\tau), \tau) = f_i(\tau), \quad i = \overline{0, N+1}.$$

Since it is necessary in the course of the test to determine the displacements of the sensors relative to each other, then one of them can be regarded as the origin of a new coordinate system. Thus, the measurement data can be represented in the form:

Translated from Inzhenerno-Fizicheskii Zhurnal, Vol. 56, No. 6, pp. 1001-1008, June, 1989. Original article submitted January 6, 1988.

0022-0841/89/5606-0707$12.50

$$T_{\text{expt}}(X_i(\tau),\ \tau) = f_i(\tau),\ i = \overline{0,\ N+1},$$
$$X_0(\tau) = 0,\ X_i(\tau) = Y_i(\tau) - Y_0(\tau),\ i = \overline{1,\ N},$$
$$X_{N+1}(\tau) = Y_{N+1}(\tau) - Y_0(\tau) = b(\tau).$$

Using the readings of the first and last sensor as first-order boundary conditions and designating $f_0(\tau) = g_1(\tau)$ and $f_{N+1}(\tau) = g_2(\tau)$, we formulate the inverse problem of determining the temperature dependence of effective thermal conductivity as follows. We need to determine the function $\lambda(T)$ and temperature field $T(x, \tau)$ that satisfy the boundary-value problem:

$$C(T)\frac{\partial T}{\partial \tau} = \frac{\partial}{\partial x}\left(\lambda(T)\frac{\partial T}{\partial x}\right),\ x \in (0,\ b(\tau)),\ \tau \in (0,\ \tau_m], \tag{1}$$

$$T(x,\ 0) = T_0(x),\ x \in [0,\ b(0)], \tag{2}$$

$$T(0,\ \tau) = g_1(\tau),\ \tau \in (0,\ \tau_m], \tag{3}$$

$$T(b(\tau),\ \tau) = g_2(\tau),\ \tau \in (0,\ \tau_m], \tag{4}$$

as well as the auxiliary conditions:

$$\begin{gathered} T(X_i(\tau),\ \tau) = f_i(\tau),\ i = \overline{1,\ N},\ \tau \in (0,\ \tau_m],\ X_i(\tau) \in (0,\ b(\tau)), \\ X_{i-1}(\tau) < X_i(\tau),\ \ i = \overline{1,\ N},\ X_0(\tau) = 0,\ X_{N+1}(\tau) = b(\tau), \end{gathered} \tag{5}$$

where $C(T)$; $T(x)$; $g_1(\tau)$; $g_2(\tau)$; $f_i(\tau)$; $i = \overline{1,\ N}$; $X_i(\tau)$; $i = \overline{1,\ N+1}$ are known functions.

We will use the method in [6] to construct the algorithm for solving inverse problems (1-5). We introduce an error functional characterizing the standard deviation of the temperatures at the sensor locations calculated with model (1-4) from the experimentally-measured values. We then attempt to establish the function $\lambda(T)$ from the condition

$$J(\lambda(T)) = \sum_{i=1}^{N}\int_0^{\tau_m}[T(X_i(\tau),\ \tau,\ \lambda(T)) - f_i(\tau)]^2\,d\tau \simeq \delta^2, \tag{6}$$

where δ^2 is an assigned level of error determined from analysis of the measurement errors.

The inverse probelm consists of solving approximate equation (6) for $\lambda(T)$ with allowance for conditions (1-4).

We represent the sought function $\lambda(T)$ on the interval $[T_{\min},\ T_{\max}]$ in parametric form, where $T_{\min}$ and $T_{\max}$ are the minimum and maximum values of temperature in the specimen region being examined. We use cubic B-splines [7] for the parameterization and we seek the function $\lambda(T)$ in the form

$$\lambda(T) = \sum_{k=1}^{m}\lambda_k B_k(T),$$

where λ_k, $k = \overline{1,\ m}$ are parameters; $B_k(T)$, $k = \overline{1,\ m}$ are basis functions. As a result, the inverse problem reduces to the search for the vector of the approximation parameters $\bar{\lambda}$.

We seek the vector $\bar{\lambda}$ by minimizing the error functional. The minimization process is constructed by using the method of conjugate gradients:

$$\bar{\lambda}^{s+1} = \bar{\lambda}^s + \alpha^s \bar{G}^s,\ \ s = 0,\ 1,\ 2,\ \ldots,\ s^*,$$

where

$$\bar{G}^s = -(\bar{J}'_\lambda)^s + \beta^s \bar{g}^{s-1};$$

$$\beta^0 = 0,\ \ \beta^s = \langle (\bar{J}'_\lambda)^s - (\bar{J}'_\lambda)^{s-1};\ (\bar{J}'_\lambda)^s \rangle_{R^M} / \| (J'_\lambda)^{s-1} \|_{R^M};$$

s* is the number of the iteration at which Eq. (6) is satisfied. The depth of descent α is chosen from the condition

$$\min_{\alpha^s \in R^+} (J(\bar{\lambda}^{s+1} + \alpha^s \bar{G}^s)).$$

The gradient of the functional being minimized is calculated from the formula

$$J'_{\lambda_k} = \sum_{i=1}^{N+1} \int_0^{\tau_m} \int_{X_{i-1}(\tau)}^{X_i(\tau)} \psi_i \left(\frac{\partial^2 T}{\partial x^2} B_k(T) + \left(\frac{\partial T}{\partial x} \right)^2 \frac{\partial B_k}{\partial T}(T) \right) dx d\tau, \quad k = \overline{1, m},$$

where $\psi_i(x, \tau)$ is the solution of the boundary-value problem conjugate with the initial problem (1-4):

$$-C \frac{\partial \psi_i}{\partial \tau} = \lambda \frac{\partial^2 \psi_i}{\partial x^2}, \quad x \in (X_{i-1}(\tau), \quad X_i(\tau)), \quad \tau \in (0, \tau_m],$$

$$\psi_i(x, \tau_m) = 0, \quad x \in [X_{i-1}(\tau), X_i(\tau)], \quad i = \overline{1, N+1},$$

$$\psi_1(0, \tau) = 0, \quad \tau \in [0, \tau_m),$$

$$\psi_{N+1}(X_{N+1}(\tau), \tau) = 0, \quad \tau \in [0, \tau_m),$$

$$\psi_i(X_i(\tau), \tau) = \psi_{i+1}(X_i(\tau), \tau), \quad \tau \in [0, \tau_m), \quad i = \overline{1, N},$$

$$\frac{\partial \psi_i}{\partial x}(X_i(\tau), \tau) - \frac{\partial \psi_{i+1}}{\partial x}(X_i(\tau), \tau) = \frac{2}{\lambda}(T(X_i(\tau), \tau) - f_i(\tau)),$$

$$\tau \in [0, \tau_m), \quad i = \overline{1, N}.$$

To determine the depth of descent, we use its linear estimate

$$\alpha_s = -\sum_{i=1}^{N} \int_0^{\tau_m} (T(X_i(\tau), \tau) - f_i(\tau)) \vartheta_i(X_i(\tau), \tau) d\tau \Big/ \sum_{i=1}^{N} \int_0^{\tau_m} (\vartheta_i(X_i(\tau), \tau))^2 d\tau,$$

where $\vartheta_i(x, \tau)$ is the solution of the following boundary-value problem:

$$C \frac{\partial \vartheta_i}{\partial \tau} = \lambda \frac{\partial^2 \vartheta_i}{\partial x^2} + 2 \frac{\partial \lambda}{\partial T} \frac{\partial T_i}{\partial x} \frac{\partial \vartheta_i}{\partial x} + \left(\frac{\partial^2 T}{\partial x^2} \frac{\partial \lambda}{\partial T} + \right.$$

$$\left. + \left(\frac{\partial T}{\partial x} \right)^2 \frac{\partial^2 \lambda}{\partial T^2} - \frac{\partial T}{\partial \tau} \frac{\partial C}{\partial T} \right) \vartheta_i + \left(\sum_{k=1}^{M} G_k B_k(T) \right) \frac{\partial^2 T}{\partial x^2} + \left(\frac{\partial T}{\partial x} \right)^2 \left(\sum_{k=1}^{M} G_k \frac{dB_k}{dT}(T) \right),$$

$$x \in (X_{i-1}(\tau), \quad X_i(\tau)), \quad \tau \in (0, \tau_m], \quad i = \overline{1, N+1},$$

$$\vartheta_i(x, 0) = 0, \quad x \in [X_{i-1}(0), \quad X_i(0)], \quad i = \overline{1, N+1},$$

$$\vartheta_1(0, \tau) = 0, \quad \tau \in (0, \tau_m],$$

$$\vartheta_{N+1}(X_{N+1}(\tau), \tau) = 0, \quad \tau \in (0, \tau_m],$$

$$\vartheta_i(X_i(\tau), \tau) = \vartheta_{i+1}(X_i(\tau), \tau), \quad \tau \in (0, \tau_m], \quad i = \overline{1, N},$$

$$\frac{\partial \vartheta_i}{\partial x}(X_i(\tau), \tau) = \frac{\partial \vartheta_{i+1}}{\partial x}(X_i(\tau), \tau), \quad \tau \in (0, \tau_m], \quad i = \overline{1, N}.$$

The algorithm for solving the inverse probem without allowance for the mobility of the sensors has already been examined in sufficient detail in [6]. In the numerical solution of boundary-value problems with movable boundaries, we use a coordinate transformation which leads to rectification of the fronts [8].

To experimentally study the heating and failure of materials exposed to a hot gas flow, we developed a stand which provides for nonsteady thermal loading through the movement of a high-temperature gas generator relative to a stationary holder containing the specimen. The plasma stand consists of an electric-arc plasma generator (plasmatron), systems to supply

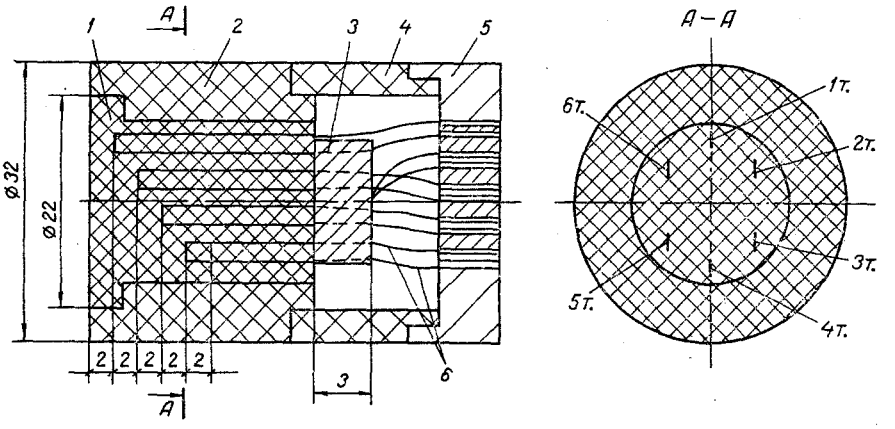

Fig. 1. Design of sensor: 1) body of sensor; 2) protective clamp; 3) calorimeter; 4) tang; 5) plug connection; 6) Chromel–alumel thermocouple.

electric power and gas, a cooling system, control panel, instrument complex, control and measuring equipment, and the test object – a block containing the specimen. The instrument complex makes it possible to obtain frame-by-frame x-ray photographs of the specimen.

The source of the hot gas flow (air) is a plasmatron with a vortically stabilized arc discharge. The working characteristics of the plasmatron: I = 300 A, power W = 89.4 kW, discharge of working gas G = 89.4 kW, discharge of working gas G = 4.8 g/sec.

The instrument complex for photographing the specimen consists of an x-ray source, a cassette with a drive, and a system to automatically control the process. The x-ray source is an RU-275 unit with ZBDM-100 tube.

The block for installing the specimen is designed so as to permit clear x-ray photographs to be taken due to the location of the casette with film near the specimen. Here, six specimen projections can be obtained by rotating it through different angles in the range 0-180° relative to its own axis.

Conducting tests to determine the parameters of the heating and failure of materials interacting with a hot gas flow, together with the use of standard specimens, requires the development of special sensors to determine the internal temperature field. After analyzing existing methods of thermocouple installation in test materials, we tried out the following design of sensor to determine temperature profiles. The specimen, made of glass-reinforced plastic on a phenol-formaldehyde binder and placed in a metallic holder with a plug connection, was a cylinder 32 mm in diameter and 70 mm high. Figure 1 shows sketches of the sensor. The protective clamp is designed to eliminate the effects of transverse heat flow. Cylindrical holes of different depth 3.5 mm in diameter are drilled in the body of the sensor at the rear. Pins with П-shaped chromel-alumel thermocouples 0.1 mm in diameter are inserted inthe holes. The thermocouples are butt-welded. The pins with attached thermocouples were previously coated with a mixture consisting of the phenol-formaldehyde resin and the filler cloth. The percentage content of components of the coating is the same as in the base material.

The distance from the end surface to the first thermocouple and between thermocouples is 2 mm. The isothermal section of thermocouples was chosen on the basis of the recommendations made in [1] for Chromel–Alumel thermocouples: $\ell/d \geq 30$, where d is the diameter of the thermocouple and ℓ is the length of the isothermal section. The depth of installation of the thermocouples was refined from the x-ray photographs. We used K-300 adhesive to attach a copper calorimeter 3 mm thick to the back side of the sensor. The temperature of the calorimeter was checked with an embedded Chromel–Alumel thermocouple.

To check for the unidimensionality of the heating conditions, we made similar heat sensors and installed several thermocouples at one depth but different distances from the symmetry axis. It was established from a comparison of the thermocouple readings that the difference in the readings was no greater than the measurement error.

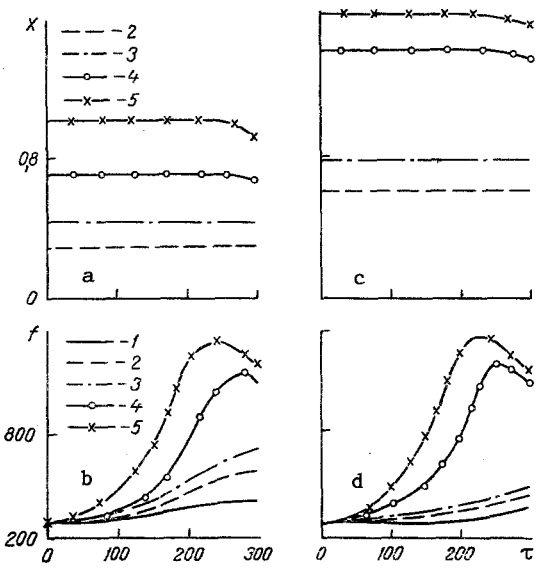

Fig. 2. Displacements X, $m \cdot 10^{-2}$, and readings of heat sensors f, K, as functions of time τ, sec: a, b) experiment No. 1; c, d) experiment No. 2; 1) left boundary; 2) first heat sensor; 3) second sensor; 4) third sensor; 5) right boundary.

The effect of shrinkage on the thermal conductivity of the material was checked in one-sided heating of the specimens. The dependence of the volumetric heat capacity of the material (glass-reinforced plastic) on temperature is shown below:

T (K) — 273	50	200	400	600	800	900
$C\left(\frac{J}{m^3 \cdot K}\right) \cdot 10^{-7}$	0,187	0,196	0,192	0,155	0,151	0,154

The initial temperature of the specimens was a constant 16°C. Five thermocouples were installed in each specimen. The readings of the two outermost thermocouples were used as known first-order boundary conditions, while the readings of the other three thermocouples were used as initial data for solving the inverse problem. Below, we analyze the results of two specimen tests. Figure 2a and b show the resulting experimental values of relative thermocouple location as a function of time in experiment No. 1. Also shown is the thermogram. Figure 2, c and d, show the same for experiment No. 2.

Before analyzing the experimental data, we conducted numerical tests which revealed that inverse problems are numerically solved most expeditiously on a grid $n_x \times n_\tau = 40 \times 40$. An important factor in analyzing the experimental data is the chosen number of parameters of the approximating B-spline. The proper choice was determined through parametric calculations performed during the solution of inverse problems, with a subsequent increase in the number of parameters of the approximation by unity until satisfaction of error condition (6). It was found that for the conditions of our experiments, the unknown relation $\lambda(T)$ is best approximated by a B-spline with the "natural" boundary conditions ($\lambda''(T_{min}) = \lambda''(T_{max}) = 0$) and four intervals of subdivision of the region in which the sought function is being approximated.

Figure 3 shows results of analysis of the test data with and without allowance for the change in thermocouple location during the experiment. In obtaining this data, we analyzed the reliability of the results. To do this, we solved the inverse problem for each case with different constant initial approximation λ^0 of the sought function. Results of such an analysis are shown in Fig. 4 for the data in experiment No. 2. The independence of the values of thermal conductivity on the quantity λ^0 is confirmation of the high degree of reliability of the results.

It is evident from Fig. 3 that for experiment No. 1 — in which the maximum thermocouple displacement was 0.15 mm — allowing for the mobility of the sensors has almost no effect on

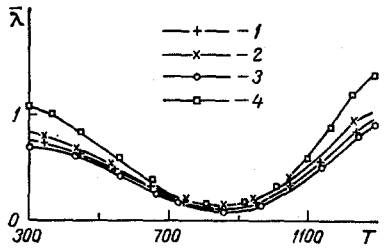

Fig. 3

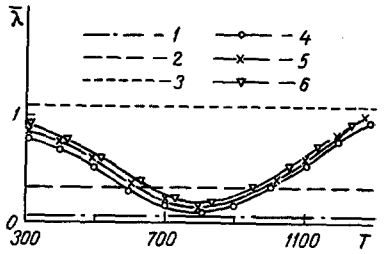

Fig. 4

Fig. 3. Determination of $\bar{\lambda}(T)$: 1) experiments Nos. 1 and 2, respectively; 3, 4) experiments Nos. 1 and 2 without allowance for the mobility of the heat sensors.

Fig. 4. Determination of $\bar{\lambda}(T)$: 1-3) different initial approximations of $\bar{\lambda}(T)$; 4-6) corresponding results of solution of the inverse heat-conduction problem.

the solution of the inverse problem. However, in experiment No. 2 – with a maximum displacement of 0.4 mm – there is a substantial difference in the estabilshed values of thermal conductivity.

The completed studies show that shrinkage of the material and the resulting displacement of the heat sensors during the experiment can sometimes significantly affect the determination of thermophysical characteristics. Thus, this factor should be taken into account when analyzing data from nonsteady thermophysical experiments.

NOTATION

T, temperature; τ, time; N, number of heat sensors; $f(\tau)$, measured values of temperature; X, Y, coordinates of the heat sensors; $g(\tau)$, temperature at the boundary of the specimen; C(T), volumetric heat capacity; $\lambda(T)$, effective thermal conductivity; τ_m, duration of experiment; $b(\tau)$, external boundary of specimen; J, error functional; δ^2, level of error; ψ, conjugate variable; α, depth of descent; ϑ, temperature increment.

LITERATURE CITED

1. Yu. V. Poleshaev and F. B. Yurevich, Thermal Protection [in Russian], Moscow (1976).
2. Yu. V. Poleshaev, V. E. Killikh, and Yu. G. Narozhnyi, Inzh.-Fiz. Zh., 29, No. 1, 39-44 (1975).
3. Yu. G. Narozhnyi, Yu. V. Polezhaev, and V. N. Kirillov, Inzh.-Fiz. Zh., 29, No. 1, 77-80 (1975).
4. V. A. Strakhov, S. I. Leonov, and A. I. Garashchenko, Inzh.-Fiz. Zh., 33, No. 3, 1047-1051 (1977).
5. E. A. Artyukhin, V. E. Killikh, and A. A. Okhapkin, Inzh.-Fiz. Zh., 45, No. 5, 788-794 (1983).
6. E. A. Artyukhin, Teplofiz. Vys. Temp., 19, No. 5, 963-967 (1981).
7. S. B. Stechkin and Yu. N. Subbotin, Splines in Computational Mathematics [in Russian], Moscow (1976).
8. F. P. Vasil'ev, Zh. Vychisl. Mat. Mat. Fiz., 3, No. 5, 861-873 (1963).